PoS PROCEEDINGS OF SCIENCE

SMOG: a high-density gas target experiment at LHCb

Chiara Lucarelli[a,*] **on behalf of the LHCb collaboration**

[a] *Università degli studi e INFN Firenze,*
Via Sansone, 1, 50019 Sesto Fiorentino (FI), Italy

E-mail: chiara.lucarelli@cern.ch

Owing to the injection of gas into the LHC beampipe while multi-TeV proton or ion beams are circulating, the LHCb spectrometer has the unique capability to function as the as-of-today highest-energy fixed-target experiment. The resulting beam-gas collisions cover an unexplored energy range that is above previous fixed-target experiments, but below RHIC or LHC collider energies. Here we present recent results for hadron production and polarization from beam-gas fixed-target collisions at LHCb. Also, the upgrade of the fixed-target system, named SMOG2, and the preliminary results from the first collected data, are discussed.

42nd International Conference on High Energy Physics (ICHEP2024)
18-24 July 2024
Prague, Czech Republic

*Speaker

1. LHCb fixed-target programme

The LHCb experiment is a general purpose experiment on the LHC ring, characterised by a single-arm spectrometer covering the forward pseudorapidity $\eta \in [2, 5]$ [1]. In addition to its distinctive kinematic coverage, the LHCb detector has the unique possibility at the LHC to operate also as the highest-energy fixed-target experiment. This is made possible by the gas injection system SMOG, originally designed to inject gases in the accelerator beam-pipe to perform precise luminosity measurements. Since 2015, leveraging the forward geometry of the detector and its excellent tracking and particle identification performance, samples with both proton and lead-ion beams were collected injecting noble gases (He, Ne, Ar), covering a rapidity region in the centre of mass system ($-3 < y^* < 0$) complementary to those covered by the collider mode samples. This configuration provides unique physics opportunities at the LHC. SMOG allows access to the high Bjorken-x and moderate Q^2 region, mostly unexplored by previous experiments. Moreover, nuclei with atomic numbers between the proton and lead can be studied, providing insights to several research topics including nuclear structure, heavy flavour production, and even Cosmic Rays physics (Fig. 1) [2].

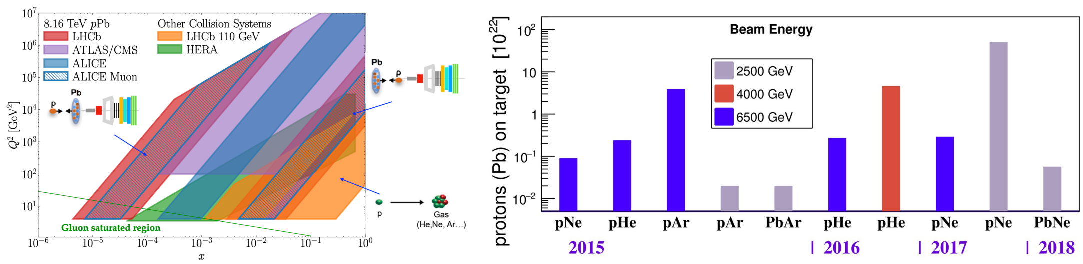

Figure 1: The LHCb acceptance in the Q^2/ Bjorken-x plane compared to other experiments (left) and the integrated luminosity of the samples collected with SMOG between 2015 and 2018, indicating the collision system, the energy and the statistics as p (Pb) on target (right).

2. Antimatter production for Cosmic Rays physics

The antiproton $\bar{p}$ production in pHe collisions represents a crucial ingredient to constrain the $\bar{p}$ flux produced by Cosmic Rays spallation on the InterStellar Medium, mainly composed of hydrogen and helium. Indeed, the knowledge of this secondary production, background to dark matter decay or annihilation searches, is currently the main limitation to the interpretation of the $\bar{p}$ flux data collected by space-based experiments, such as AMS-02 [3]. The first-ever measurements of prompt antiproton production in pHe were performed by LHCb in 2018 [4], exploiting the injection of helium through SMOG. While the results already contributed to improvements in the modelling of secondary $\bar{p}$ production in space, the "detached" contribution of $\bar{p}$ produced from anti-hyperon decays constitutes around 20% of the total abundance and it was addressed in a separate measurement [5]. The detached-to-prompt $\bar{p}$ production ratio has been measured using two complementary approaches, exploiting the prompt result in the ratio. In the exclusive approach, the dominant contribution coming from the $\bar{\Lambda} \to \bar{p}\pi^+$ is reconstructed without the use of any particle identification information. An inclusive approach is also considered, exploiting the excellent particle identification performance and impact parameter resolution. The $\bar{p}$ candidates, identified using the Ring Imaging Cherenkov detectors, are distinguished between promptly and decay-produced based on each candidates' consistency with originating from the pHe collision point. Both approaches highlight a larger contribution in the ratio with respect to the predictions of the most commonly used theoretical models (Fig. 2). The ratio between the exclusive and inclusive results is also compared to the EPOS-LHC [6] prediction, which is expected to be reliable for this quantity since it only depends on the s-quark hadronization. The observed consistency confirms the validity of the two approaches.

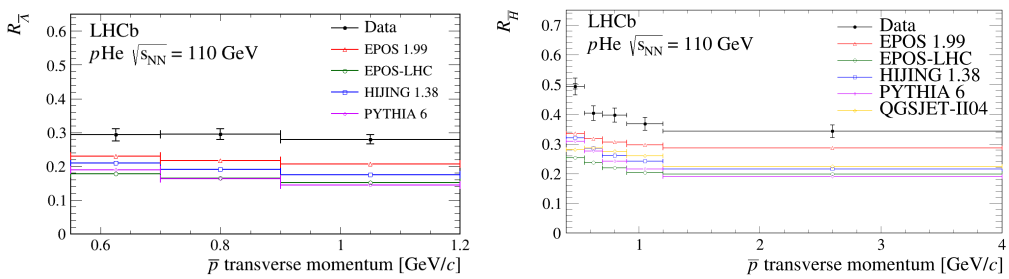

Figure 2: Results for the detached-to-prompt antiproton ratio measurement as a function of the transverse momentum. Both the exclusive (left) and inclusive (right) approaches show an excess with respect to the predictions.

3. Charm production in pNe and PbNe

Quarkonia dissociation due to colour charge screening is a mechanism predicted by Quark-Gluon Plasma (QGP) theories. Its observation requires precise knowledge of the concurrent initial and final state effects, known as Cold Nuclear Matter (CNM) effects. Measuring charm production in different collision systems and energies is therefore crucial to constrain the CNM effects and to shed light on QGP formation. Recently, LHCb measured D^0, J/ψ, and $\psi(2s)$ production in pNe [7, 8] and PbNe [9] collisions both with $\sqrt{s_{\rm NN}}$ = 68 GeV. Exploiting the fixed-target configuration, the results cover an unexplored energy scale, and thanks to the high-x coverage, they are sensitive to a possible intrinsic charm contribution to the proton parton distribution functions. The J/ψ differential cross-section as a function of the centre-of-mass rapidity $y*$ are found to be in excess with respect to predictions considering the color singlet model (Fig. 3, left). When compared to models considering color evaporation and contributions from nuclear absorption and multiple scattering [10], the agreement is good but it is not discriminating enough to identify the possible presence of intrinsic charm. Thanks to the available large pNe sample size, the $\psi(2s)$ has also been studied. In particular, Fig. 3, centre, shows the $\psi(2s)$-to-J/ψ ratio from measurements with similar target masses, where an agreement with previous experiments is found. Finally, Fig. 3, right, presents the PbNe results. They represent the unique opportunity at LHC to measure the J/ψ-to-D^0 ratio correcting for CNM effects, exploiting the measurement performed in the pNe sample. The QGP formation would be highlighted as a change in the exponential between the pNe and the central PbNe events in the distribution of the ratio as a function of the centre-of-mass rapidity (number of binary nucleon-nucleon collisions N_{coll}, obtained applying the Glauber model to the energy deposits in the calorimeter). While additional nuclear effects are highlighted for the J/ψ, there is no evidence for anomalous suppression at this level of precision.

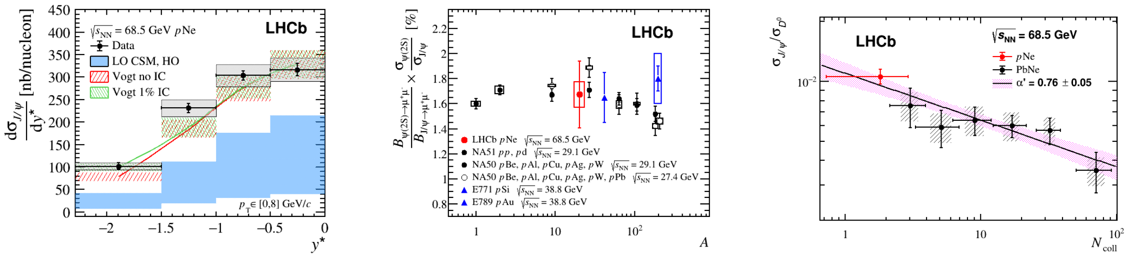

Figure 3: Left: the differential cross-section for J/ψ in pNe collisions as a function of $y*$ is compared to several theoretical models. Centre: the $\psi(2s)$-to-J/ψ ratio in pNe collisions is compared to measurements from other fixed-target experiments. Right: the J/ψ-to-D^0 ratio as a function of the number of binary nucleon-nucleon collisions N_{coll}

4. Λ transverse polarization in pNe collisions

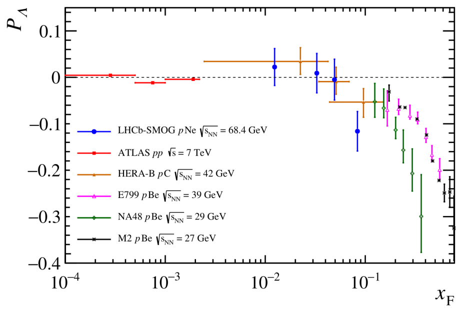

Figure 4: Comparison of the magnitude of the Λ hyperson polarization as a function of x_{F} obtained in the experiments performed up to the time of writing.

The spontaneous transverse polarization of Λ hyperons was first observed in 1976 in inclusive production by an unpolarized 300 GeV proton beam on a beryllium target [11]. Following a phenomenological approach, the polarizing fragmentation function $D_{1T}^{\perp}$ has been proposed to account for the polarization of the Λ. Following the same approach used in the framework of the transverse-momentum-dependent (TMD) fragmentation functions, $D_{1T}^{\perp}$ describes the fragmentation of an unpolarized quark into a transversely polarized hadron accounting for spin and momentum correlations [12]. In order to determine this function, several experiments have been performed covering a wide range in centre-of-mass energies and collision systems. LHCb performed the Λ transverse polarization measurement considering the pNe sample at $\sqrt{s_{\mathrm{NN}}} = 68$ GeV [13]. The polarization is measured exploiting the strong parity violation of the decays of the $\Lambda \to p\pi^-$ and $\bar{\Lambda} \to \bar{p}\pi^+$. Indeed, considering the Λ rest frame, the angular distribution of the products show a large asymmetry and the proton is preferentially emitted along the direction of the spin of the Λ:

$$\frac{dN}{d\cos\theta} = \frac{dN_0}{d\cos\theta}\left(1 + \alpha P_{\Lambda}\cos\theta\right), \tag{1}$$

where θ is the angle between the proton momentum and the normal to the production plane, $\frac{dN_0}{d\cos\theta}$ is the decay distribution for unpolarized Λ hyperons, P_Λ is the magnitude of the polarization, and α is the value of the parity-violating decay asymmetry for the Λ hyperon. The magnitude of the polarization is obtained from the linear fit to the angular distribution of the proton, where α is fixed to the world average. The final polarizations obtained are $P_\Lambda = 0.029 \pm 0.019$ (stat) $\pm\, 0.012$ (syst) and $P_{\bar{\Lambda}} = 0.003 \pm 0.023$ (stat) $\pm\, 0.014$ (syst) for the Λ and $\bar{\Lambda}$, respectively. When compared to earlier experiments, the polarization results as a function of the Feynman-x variable x_F are in agreement, in particular with with HERA-B results, which cover a similar x_F range (Fig. 4).

5. LHCb fixed-target Run3 upgrade

Since 2022, an upgrade of the fixed-target system, called SMOG2, has been operational, collecting data simultaneously with the pp physics programme [14]. A 20 cm-long storage cell has been installed 44 cm upstream of the nominal LHCb interaction point and a new gas feed system allows for precise control of the gas flow, pressure, and injected species. Leveraging the reduced interaction region, a two-order-of-magnitude increase in instantaneous luminosity has been achieved, and new non-noble gases, such as hydrogen (H_2), deuterium (D_2) and oxygen (O_2), can be injected. Moreover, the separation between the beam-beam and beam-gas collision regions offers the unique opportunity at LHC to simultaneously collect data both in collider and fixed-target mode exploiting all the bunches. LHCb is therefore the only experiment at the LHC able to operate with two different interaction systems and centre-of-mass energies at the same time. An example of preliminary results obtained with the data collected during 2024 can be observed in Fig. 5. On the left, the recorded integrated luminosity for gas species at the time of writing is shown. The right figure shows an example of the invariant mass distribution of reconstructed $D^0 \to K^-\pi^+$ candidates in the data-taking periods with simultaneous $pp + p$Ar collisions [**?**]. In a data acquisition period of around 100 hours of injection, more than one million D^0 candidates were reconstructed. A very large sample of charm hadrons can therefore be expected from the SMOG2 system. The upgraded fixed-target system will therefore contribute to a “significant extension of the LHC complex physics reach at a limited cost”, as highlighted in the 2020 European Strategy for Particle Physics Update [16].

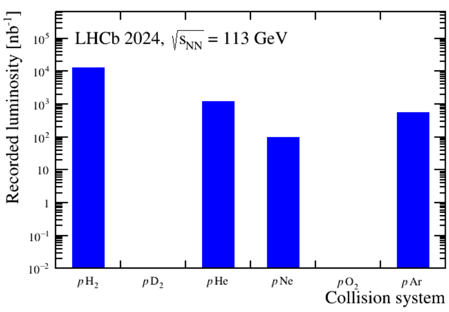

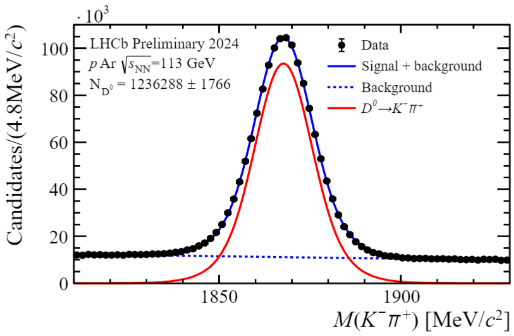

Figure 5: The left plot shows the integrated luminosity recorded at the date of writing. The right plot shows the invariant mass distribution for $D^0 \to K^-\pi^+$ decay candidates, collected over around 100 hours of injection.

References

[1] Aaij, R. et al., The LHCb Detector at the LHC, JINST **3**, 08 S08005 (2008)

[2] Bursche, A. et al., Physics opportunities with the fixed-target program of the LHCb experiment using an unpolarized gas target, CERN-LHCb-PUB-2018-015 (2018).

[3] Giesen, G. et al., AMS-02 antiprotons, at last! Secondary astrophysical component and immediate implications for Dark Matter, JCAP **09**, 023 (2015)

[4] Aaij, R. et al., Measurement of Antiproton Production in pHe Collisions at $\sqrt{s_{\rm NN}}$ = 110 GeV, Phys. Rev. Lett. **121**, 22 222001 (2018)

[5] Aaij, R. et al., Measurement of antiproton production from antihyperon decays in pHe collisions at $\sqrt{s_{\rm NN}}$ = 110 GeV, Eur. Phys. J. C **83**, 6 543 (2023)

[6] Pierog, T. et al., EPOS Model and Ultra High Energy Cosmic Rays, Nucl Phys B **196**, 102-105 (2009)

[7] Aaij, R. et al., Charmonium production in pNe collisions at $\sqrt{s_{\rm NN}}$ = 68.5 GeV, Eur. Phys. J. C **83**, 7 625 (2023)

[8] Aaij, R. et al., Open charm production and asymmetry in pNe collisions at $\sqrt{s_{\rm NN}}$ = 68.5 GeV, Eur. Phys. J. C **83**, 6 541 (2023)

[9] Aaij, R. et al.,J/ψ and D^0 production in $\sqrt{s_{\rm NN}}$ = 68.5 GeV PbNe collisions, Eur. Phys. J. C **83**, 7 658 (2023)

[10] Vogt, R., Limits on intrinsic charm production from the SeaQuest experiment, Phys. Rev. C **103**, 3 035204 (2021)

[11] Bunce, G. et al., Λ^0 Hyperon Polarization in Inclusive Production by 300-GeV Protons on Beryllium, Phys. Rev. Lett. **36**, 19 1113–1116 (1976)

[12] Boer, D. et al., Spin asymmetries in jet-hyperon production at LHC, Physics Letters B **659**, 1 127-136 (2008)

[13] Aaij, R. et al., Transverse polarization measurement of Λ hyperons in pNe collisions at $\sqrt{s_{NN}}$ = 68.4 GeV with the LHCb detector. Submitted to JHEP (2024). arXiv:2405.11324

[14] Boente Garcia, O., A high-density gas target at the LHCb experiment. Submitted to Physical Review Accelerators and Beams (2024). arXiv:2407.14200

[15] Aaij, R. et al., Charm results in SMOG2 2024 data. LHCb-FIGURE-2024-023 (2024).

[16] Ellis, R. K. et al., Physics Briefing Book: Input for the European Strategy for Particle Physics Update 2020. CERN-ESU-004 (2019).